Electronic Supplementary Information (ESI):

Nitrogen-doped porous carbon derived from bimetallic metal-organic framework as highly efficient electrodes for flow-through deionization capacitors

Zhuo Wang, Tingting Yan, Jianhui Fang, Liyi Shi and Dengsong Zhang*

*Department of Chemistry, Research Center of Nano Science and Technology, Shanghai University, Shanghai 200444, China. Fax: 86 21 66136079; *E-mail: dszhang@shu.edu.cn*

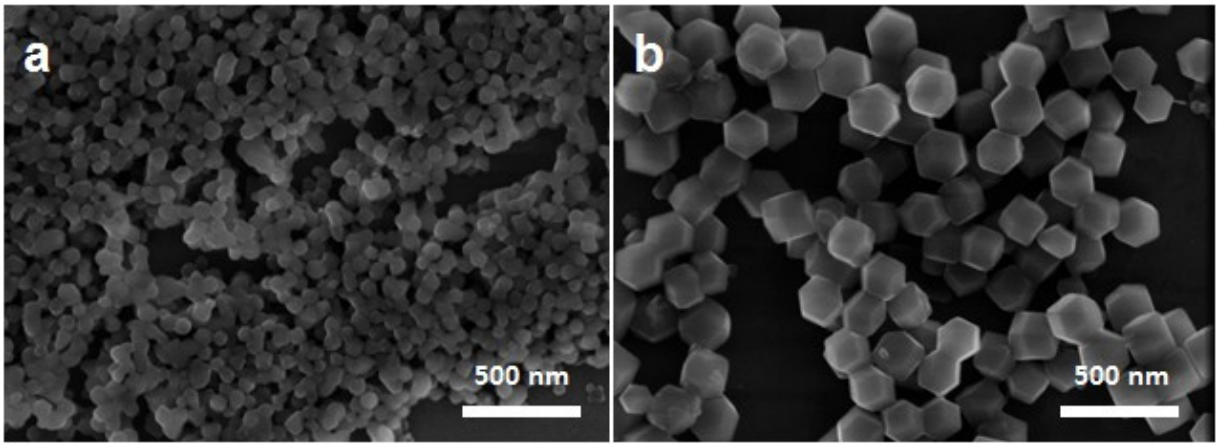

Fig. S1 SEM images of ZIF-8 (a) and ZIF-67 (b).

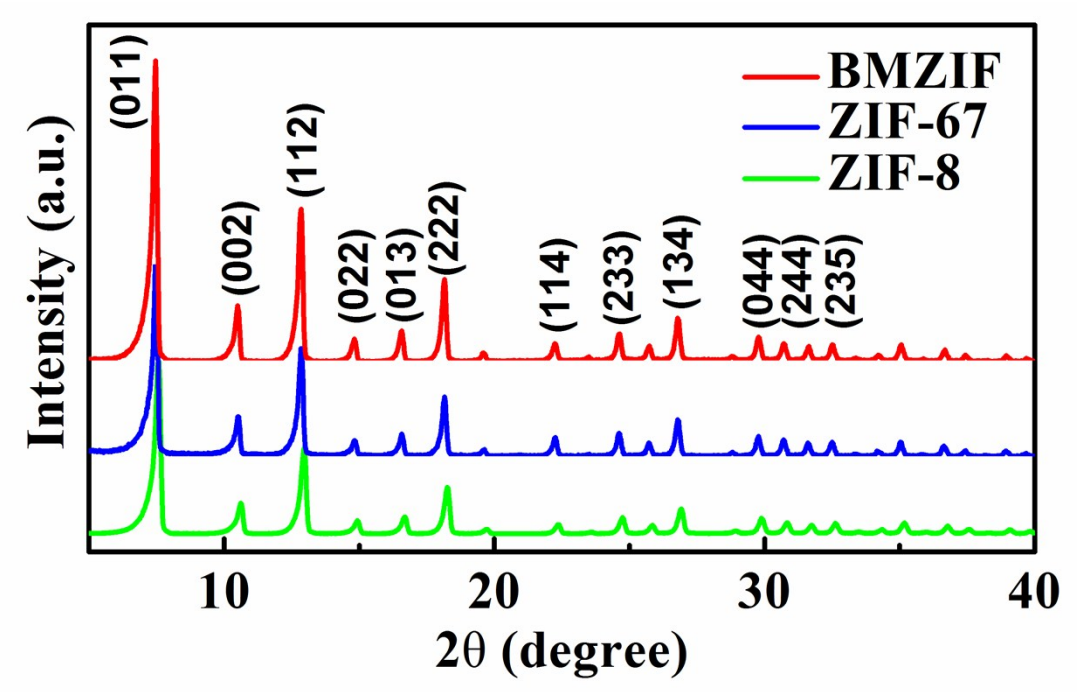

Fig. S2 Wide-angle XRD patterns of as-synthesized ZIF-8, ZIF-67, and BMZIF crystals.

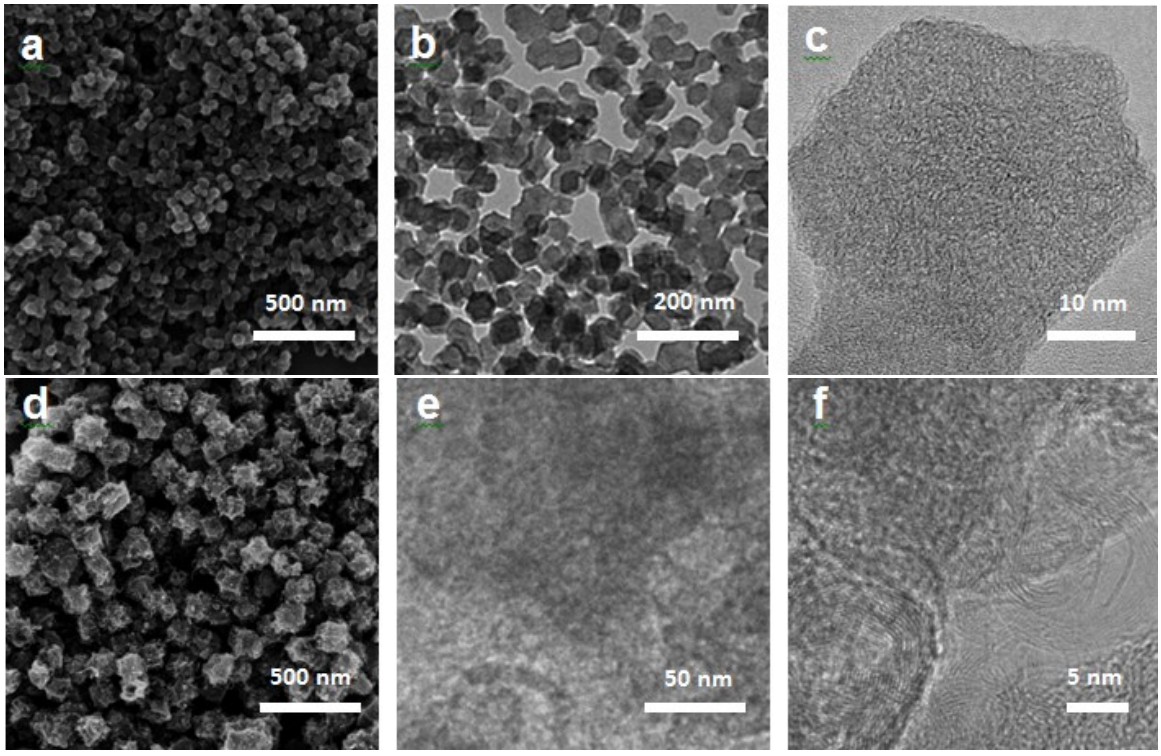

Fig. S3 SEM images (a, d), TEM images (b, e), and HRTEM images (c, f) of NC (a-c) and GC (d-f).

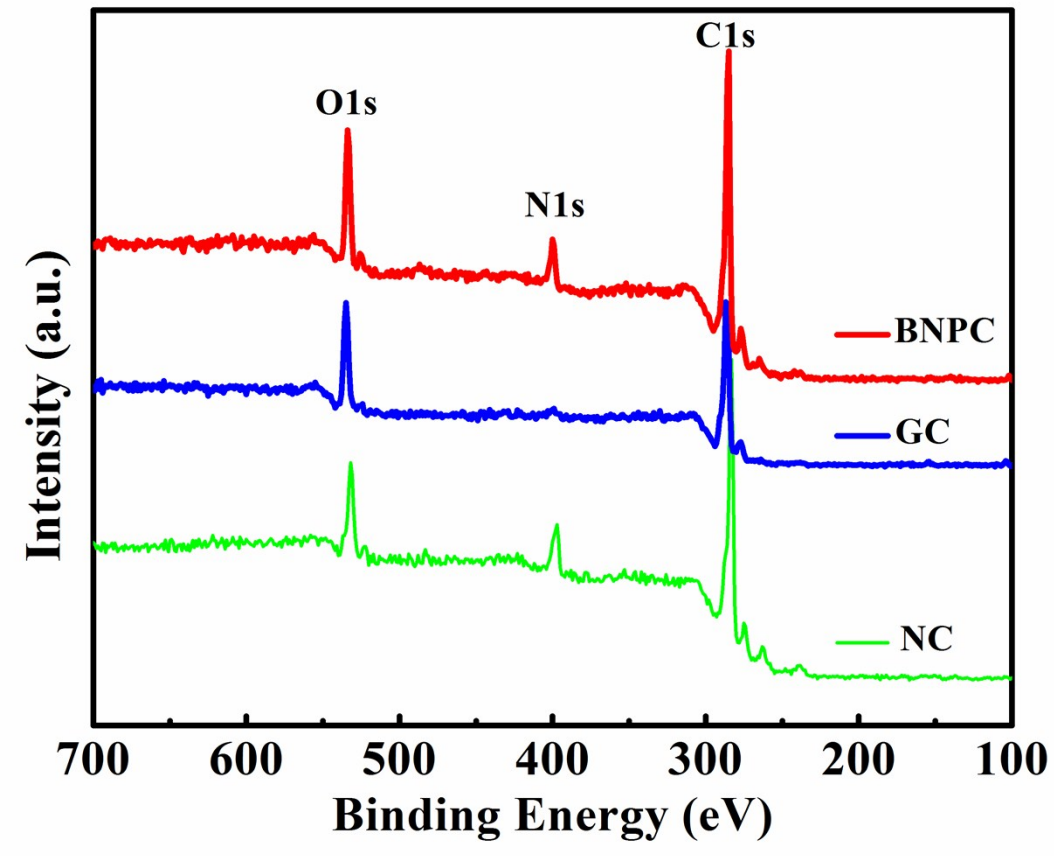

Fig. S4 XPS survey spectra of BNPC, NC, and GC samples.

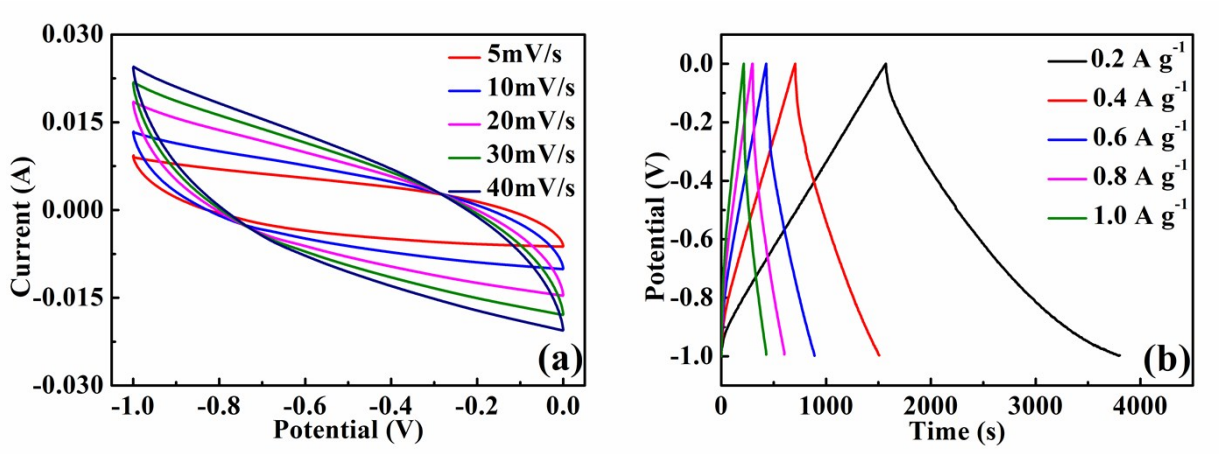

Fig. S5 Electrochemical performance of the BNPC electrode measured in a three-electrode system: (a) CV curves at various scan rates and (b) the galvanostatic charge/discharge curves at various current densities. All the curves were obtained in a 0.5 M NaCl solution.

Table S1. The specific capacitances (F g^{-1}) of the samples obtained from discharge curve in the three-electrode system.

Sample	0.2 A g^{-1}	0.4 A g^{-1}	0.6 A g^{-1}	0.8 A g^{-1}	1.0 A g^{-1}
BNPC	532.18	329.84	275.21	247.06	226.71
NC	493.25	318.14	265.54	236.07	212.26
GC	398.73	268.90	241.23	219.82	205.63

Table S2. The specific capacitances of the samples obtained from discharge curve in the two-electrode system.

Sample	0.2 A g^{-1}	0.4 A g^{-1}	0.6 A g^{-1}	0.8 A g^{-1}	1.0 A g^{-1}
BNPC	395.00	313.69	292.12	285.97	291.47
NC	372.17	306.54	286.22	280.68	274.45
GC	349.47	266.57	246.14	236.54	239.54

The capacitance performances of the samples were also evaluated in a two electrode system at room temperature. The preparation of thin film electrode is similar to that described in the experimental section. A symmetrical two-electrode electrochemical cell was fabricated with 0.5 M NaCl aqueous solution as electrolyte. The mass of active materials on each electrode was 2.5 mg. The cyclic voltammetry and galvanostatic charge-discharge measurements were carried out with a potential window from -1.0 to 0 V. The specific capacitances were obtained from the CV curves by the following equation:[1-3]

$$C = \frac{Q}{U \times m} \times 4$$

where C is the specific capacitance, m is the total mass of the active materials on the two electrodes, the multiplier of 4 adjusts the capacitance of the cell and the combined mass of two electrodes to the capacitance and mass of a single electrode, Q is the integrated voltammetric charge, and U is the voltage range of cyclic voltammogram. The specific capacitance is also calculated from the discharge curves according to the following equation:[1-3]

$$C = \frac{I \times \Delta t}{\Delta V \times m} \times 4$$

where I is the discharge current, Δt is the discharge time, ΔV is the voltage change (excluding the iR drop) within the discharge time, and m is the total mass of the active materials on on both electrodes.

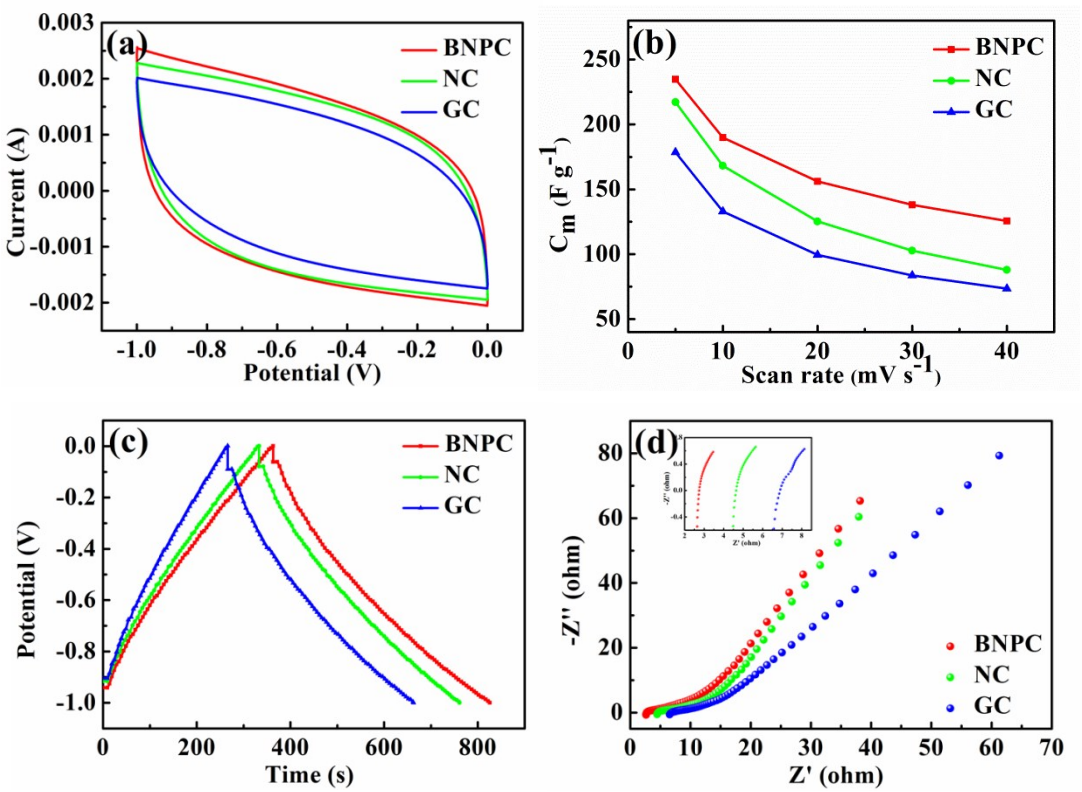

Fig. S6 Electrochemical properties of the BNPC, NC, and GC electrodes in a two-electrode system. (a) Cyclic voltammograms at a scan rate of 5 mV s^{-1}, (b) specific capacitance at different scan rates, (c) Galvanostatic charge/discharge curves at a current density of 200 mA g^{-1}, and (d) the Nyquist plots, inset shows the high-frequency region of the plot. All the curves were obtained in a 0.5 M NaCl solution.

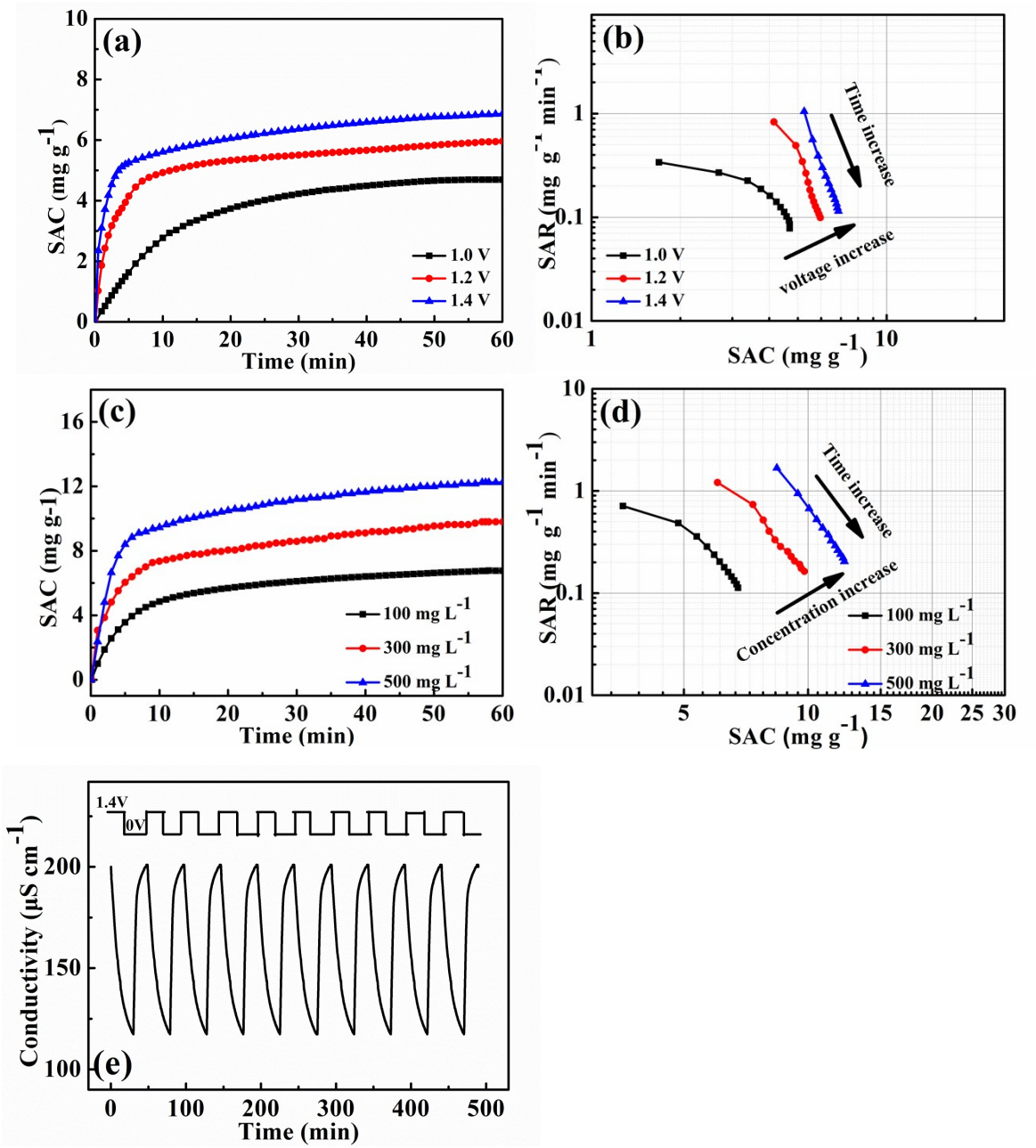

Fig. S7 (a, c) the SAC curves and (b, d) FTDC Ragone plots for the NC electrode at different cell voltages (a, b) and in different concentrations of NaCl solution (c, d). (e) Regeneration performance of the NC electrode in a 100 mg L^{-1} NaCl solution at a cell voltage of 1.4 V.

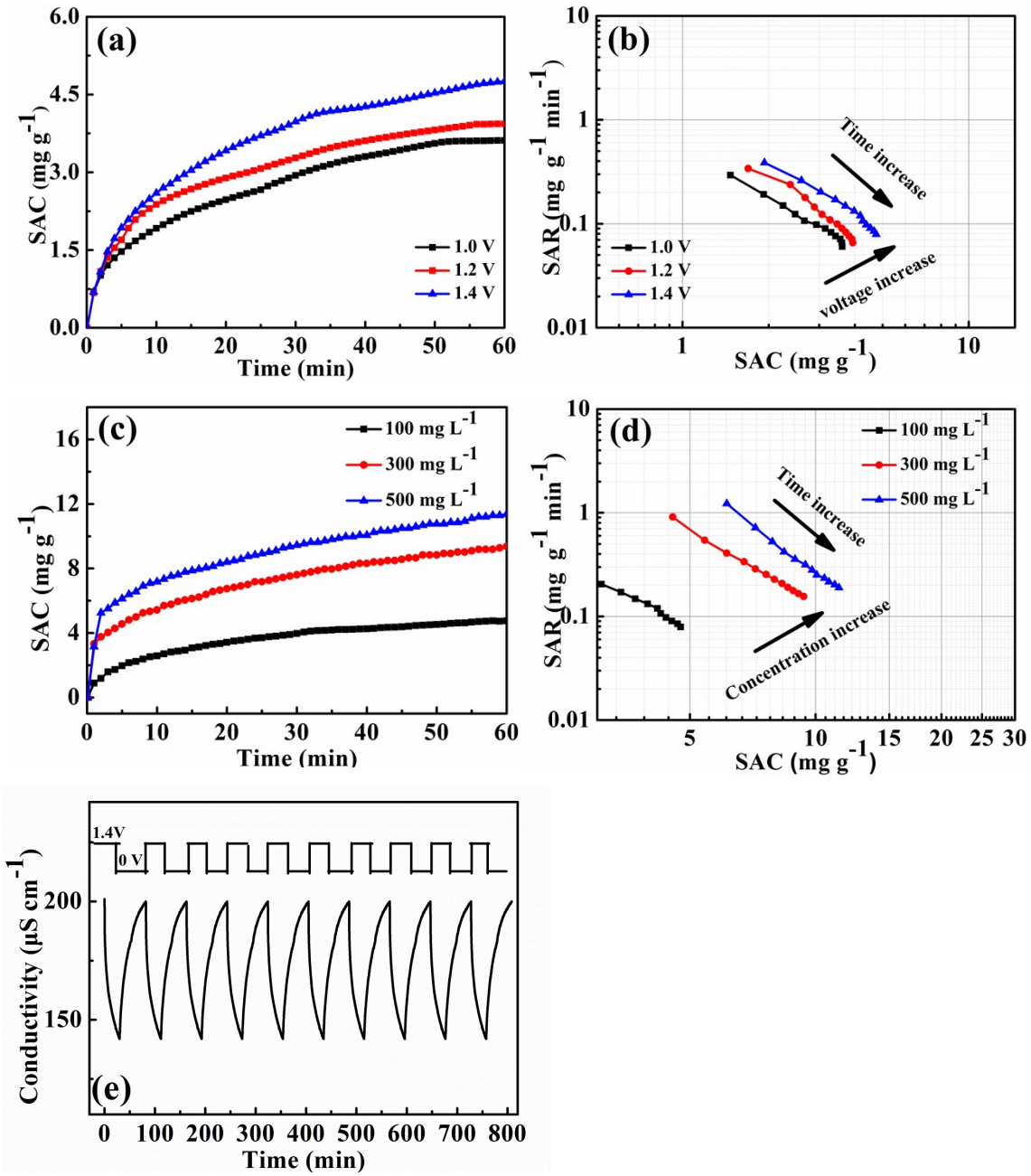

Fig. S8 (a, c) the SAC curves and (b, d) FTDC Ragone plots for the GC electrode at different cell voltages (a, b) and in different concentrations of NaCl solution (c, d). (e) Regeneration performance of the GC electrode in a 100 mg L^{-1} NaCl solution at a cell voltage of 1.4 V.

Table S3. Comparison of SAC of various carbon electrode materials from the literature.

Electrode material	**Applied voltage (V)**	**Initial NaCl concentration (mg/L)**	**Salt adsorption capacity (mg/g)**	**Ref.**
carbon nanotubes	1.2	500	2.572	[4]
Carbon nanotubes	1.2	500	2.80	[5]
Graphene	1.2	50	1.85	[6]
Graphene nanosheets	2.0	250	8.6	[7]
Graphene aerogel	1.2	500	9.9	[8]
Graphene/carbon nanotube	1.6	50	0.88	[9]
Graphene/carbon nanotube	2.0	30	1.41	[10]
Graphene/mesoporous carbon	2	40	0.73	[11]
Nitrogen-doped graphene	1.8	100	4.81	[12]
Mesoporous graphene	1.6	~500	15.21	[13]
Nitrogen-doped graphene	1.8	~50	4.81	[14]
Purified graphene	1.5	~100	1.27	[15]
3D-macroporous graphene architecture	1.6	~50	3.9	[16]
3D-macroporous graphene hierarchically porous carbon	1.2	25	6.18	[17]
3D-macroporous graphene	1.2	500	14.7	[18]
3D-Graphene Architecture with Nanopores	1.6	500	15	[19]
BNPC	1.4	100	9.31	This work
BNPC	1.4	300	12.43	This work
BNPC	1.4	500	16.63	This work

References

1. M. D. Stoller and R. S. Ruoff, *Energy Environ. Sci*. 2010, **3**, 1294-1301.
2. K. Xie, X. Qin, X. Wang, Y. Wang, H. Tao, Q. Wu, L. Yang and Z. Hu, *Adv. Mater*. 2011, **24**, 347-352.
3. P. Simon and Y. Gogotsi, *Nat. Mater*. 2008, **7**, 845-854.
4. S. Wang, D. Wang, L. Ji, Q. Gong, Y. Zhu and J. Liang, *separation and purification technology*, 2007**,** **58**, 12-16
5. Y. Liu, L. K. Pan, T. Q. Chen, X. T. Xu, T. Lu, Z. Sun and D. H. C. Chua, *Electrochim Acta*, 2015, **151**, 489-496.
6. H. B. Li, T. Lu, L. K. Pan, Y. P. Zhang and Z. Sun, *J. Mater. Chem*., 2009, **19**, 6773-6779.
7. B. P. Jia and L. D. Zou, *Carbon*, 2012, **50**, 2315-2321.
8. H. Yin, S. Zhao, J. Wan, H. Tang, L. Chang, L. He, H. Zhao, Y. Gao and Z. Tang, *Advanced Materials*, 2013**, 25**, 6270-6276.
9. H. Li, S. Liang, J. Li and L. He, *Journal of Materials Chemistry A*, 2013**, 1**, 6335-6341.
10. D. S. Zhang, T. T. Yan, L. Y. Shi, Z. Peng, X. R. Wen and J. P. Zhang, *J. Mater. Chem*., 2012, 22, 14696-14704.
11. D. S. Zhang, X. R. Wen, L. Y. Shi, T. T. Yan and J. P. Zhang, *Nanoscale*, 2012, **4**, 5440-5446.
12. X. Xu, L. Pan, Y. Liu, T. Lu and Z. Sun, *Journal of Colloid and Interface Science*, 2015**, 445**, 143-150.
13. X. Gu, M. Hu, Z. Du, J. Huang and C. Wang, *Electrochimica Acta*, 2015**, 182**, 183-191.
14. X. T. Xu, L. K. Pan, Y. Liu, T. Lu and Z. Sun, *J Colloid Interf Sci*, 2015, **445**, 143-150.
15. T. N. Tuan, S. Chung, J. K. Lee and J. Lee, *Current Applied Physics*, 2015**, 15**, 1397-1401.
16. H. Wang, D. Zhang, T. Yan, X. Wen, J. Zhang, L. Shi, Q. Zhong, *J. Mater. Chem. A*, 2013, **1**, 11778-11789.
17. X. R. Wen, D. S. Zhang, T. T. Yan, J. P. Zhang and L. Y. Shi, *J. Mater. Chem. A*, 2013, **1**, 12334-12344.
18. H, Wang, T. T. Yan, P. Y. Liu, G. R. Chen, L. Y. Shi, J. P. Zhang, Q. D. Zhong and D. S. Zhang, *J. Mater. Chem. A*, 2016, **4**, 4908-4919.
19. W. Shi, H. Li, X. Cao, Z. Y. Leong, J. Zhang, T. Chen, H. Zhang and H. Y. Yang, *Scientic Reports*, 2016**, 6**, 18966.